Pressure-induced amorphous zeolitic imidazole frameworks with reduced toxicity and increased tumor accumulation improves therapeutic efficacy *In vivo*

Zhenqi Jiang[a,b,1], Yanying Li[a,b,1], Zhenni Wei[a], Bo Yuan[a], Yinjie Wang[a,b], Ozioma Udochukwu Akakuru[a,b], Yong Li[a], Juan Li[a,*], Aiguo Wu[a,**]

[a] *Cixi Institute of Biomedical Engineering, CAS Key Laboratory of Magnetic Materials and Devices, Key Laboratory of Additive Manufacturing Materials of Zhejiang Province, Ningbo Institute of Materials Technology and Engineering, Chinese Academy of Sciences, Ningbo, 315201, China*
[b] *University of Chinese Academy of Sciences, Beijing, 100049, China*

ARTICLE INFO

ABSTRACT

Zeolitic Imidazole Frameworks (ZIFs) are widely applied in nanomedicine for their high drug loading, suitable pore size, pH-responsive drug release, and so on. However, fast drug release during circulation, unexpected toxicity to mice major organs, undesirable long-term accumulation in the lung and even death currently hinder their *in vivo* biomedical applications. Herein, we report an amorphous ZIF-8 (aZIF-8) with high loading of 5-Fu through pressure-induced amorphization. This nano-system avoids early drug release during circulation and provides tumor microenvironment-responsive drug release with improved *in vitro* cell viability, and survival rate in *in vivo* evaluations as compared to ZIF-8. Furthermore, aZIF-8 shows longer blood circulation and lower lung accumulation than ZIF-8 at same injected doses. Less drug release during circulation, longer blood circulation, and better biocompatibility of aZIF-8/5-Fu significantly improves its therapeutic efficacy in ECA-109 tumor-bearing mouse, and result in 100% survival rate over 50 days after treatment. Therefore, aZIF-8 with favorable biocompatibility and long blood circulation is expected to be a promising nano-system for efficacious cancer therapy *in vivo*.

1. Introduction

As a famous porous material, zeolitic imidazole frameworks (ZIFs) have shown great potential in gas separation [1,2], catalysis [3], sensors [4,5], and drug delivery [6,7], for their tunable pore sizes, high surface areas, and structural diversity [8,9]. The high drug loading, stability during blood circulation, and pH-responsive drug release in tumor expand their application in cancer therapy [10]. For instance, ZIF-8 could deliver small molecules, nanoparticles [11], and enzymes [12,13] to tumor sites and release guests because of the decreased pH of tumor environment [14]. ZIF-8 has also been widely used in tumor imaging and therapy [15] as an ideal vehicle. However, many undesirable outcomes still hamper the *in vivo* application of ZIFs in biomedicine, such as fast drug release during circulation [7,10], unexpected toxicity to mice major organs [16], undesirable long-term

accumulation in the lung [10], and even death. Some researchers have explored surface modification [16], metal-oxide coating [17], etc., as strategies to ameliorate these side effects. Although such strategies serve to improve the biocompatibility and expand *in vivo* applications of ZIF-8, drug loading rates and pH-responsive abilities are consequently compromised. It is therefore important to explore the different states of ZIFs that could improve *in vivo* therapeutic effects.

Recently, amorphous ZIFs (aZIFs) have attracted much attention for retaining the basic connecting blocks and connectivity of ZIFs [18], but lack long-range periodic order [19,20]. aZIFs could limit the free movement of guest molecules by irreversibly collapsing porous networks through ball-milling [21], pressure [22,23], and temperature [18]. They have also shown potential application in molecule trapping [24], gas separation [25], ion transport [26], and so on. Furthermore, they are envisaged as potential candidates for drug delivery by limiting

Scheme 1. Schematic illustration of the aZIF-8/5-Fu preparation procedure and its bio-application and potential mechanism for cancer therapy. After i. v. injection of aZIF-8/5-Fu in tumor-bearing mice, aZIF-8 significantly reduces release of 5-Fu during circulation, and triggers more effective and faster 5-Fu release inside the tumor cells by its response to low pH condition.
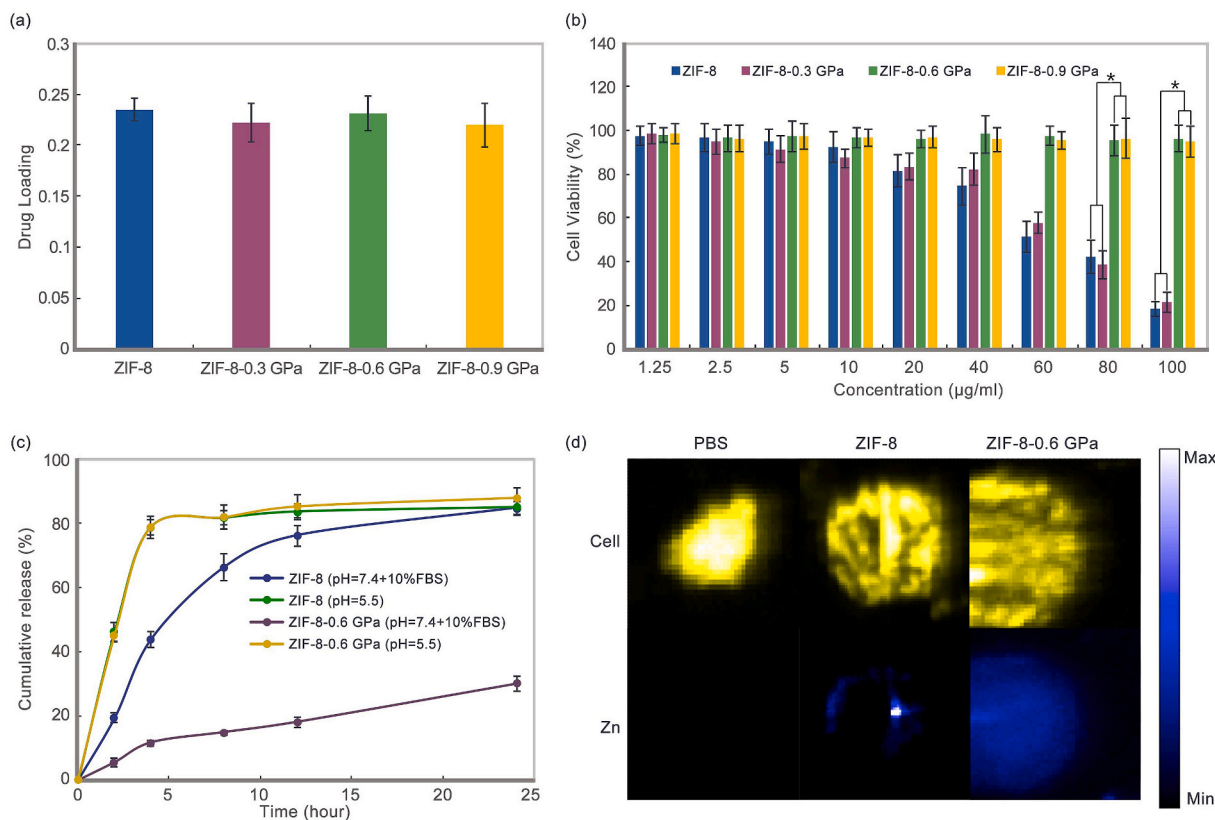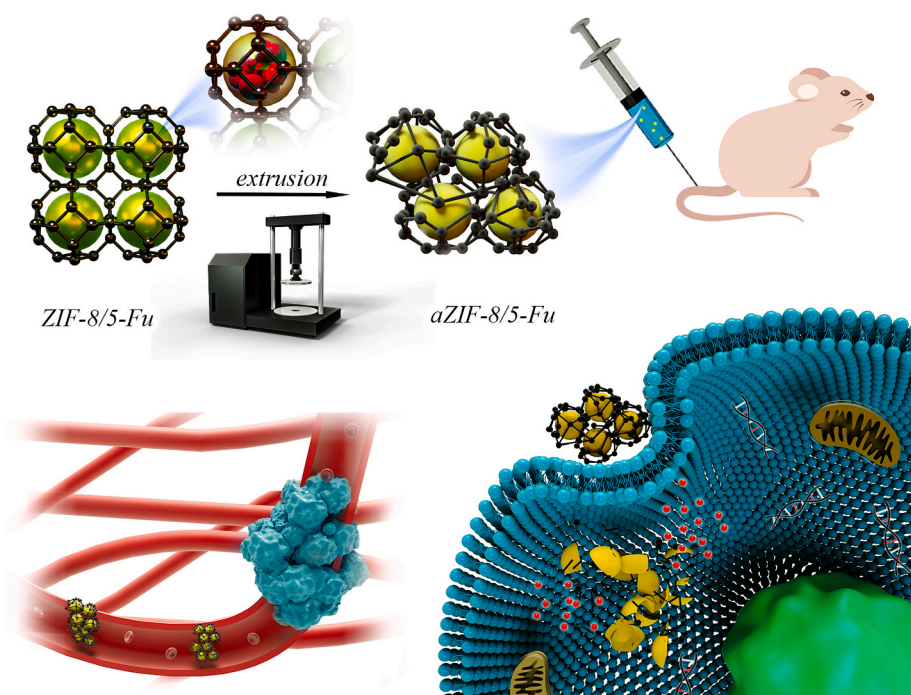
Fig. 1. (a) TEM images of ZIF-8, ZIF-8-0.3 GPa, ZIF-8-0.6 GPa, and ZIF-8-0.9 GPa; (b) XRD results, (c) FT-IR and (d) DLS results of ZIF-8, ZIF-8-0.3 GPa, ZIF-8-0.6 GPa, and ZIF-8-0.9 GPa.

the freedom of drugs [27,28]. Limiting small molecules in networks of aZIFs, which could increase stability of drugs during blood circulation, is expected to increase the therapeutic efficacy and expand the application of ZIFs in biomedicine. However, the method such as ball milling will make the particles no longer nanometers but micrometers, limiting the further application of aZIF in biomedicine [27]. Additionally,

inducing ZIF/drugs into aZIF/drugs for cancer therapy is still seldom reported. Moreover, in-depth explorations and understanding of these novel materials in nanomedicine are generally lacking.

To provide the dependable evidence that aZIFs could improve tumor therapeutic effect *in vivo*, here, aZIF-8 and fluorouracil (5-Fu)-loaded aZIF-8 nano-systems were engineered by pressure-induced
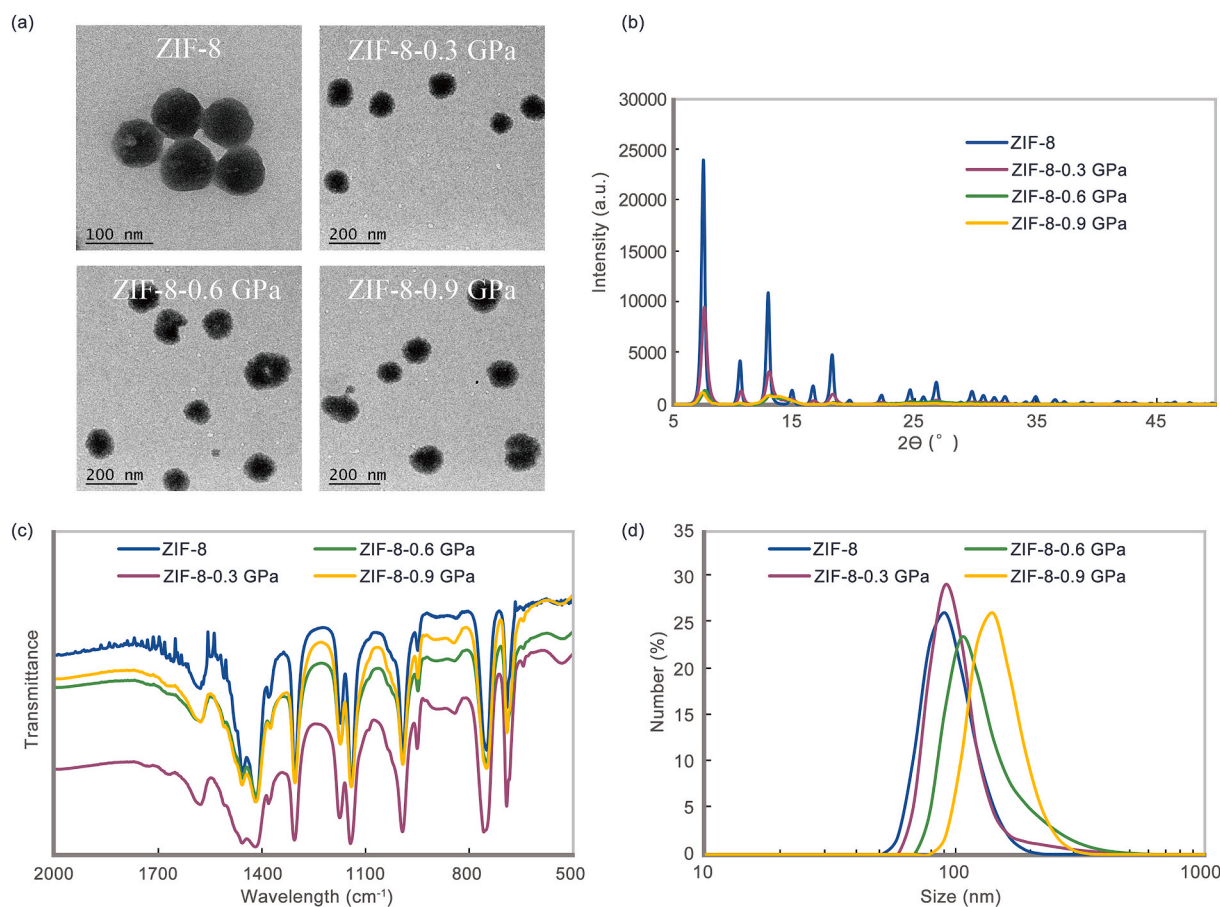
Fig. 2. (a) 5-Fu loading of ZIF-8/5-Fu after different pressure treatment. Mean ± SD (n = 3); (b) Cell viability of ECA-109 cells incubated with different samples for 24 h. Mean ± SD (n = 3), *, P < 0.05; (c) Cumulative 5-Fu release from ZIF-8 and ZIF-8-0.6 GPa in PBS (pH = 7.4 + 10% FBS and pH = 5.5) for 24 h. Mean ± SD (n = 3); (d) XFM images of Cl and Zn in ECA-109 cells incubated with ZIF-8 and ZIF-8-0.6 GPa for 4 h. The blue color bar is for Zn element.

amorphization (Scheme 1). Emphases were focused on biological functions and features of aZIFs, such as biocompatibility, biodistribution, and effectiveness as a drug delivery system especially by comparison with ZIF-8. Consequently, the improved biological functions of aZIFs were demonstrated, including prolonged controlled drug release, decreased toxicity, less pulmonary but increased tumor accumulation, and improved tumor therapy compared to ZIF-8. Taken together, this work proves that aZIF-8 with less toxicity and more accumulation in the tumor can be used as a novel nano-system for effective tumor therapy.

2. Experimental Section

2.1. Synthesis of aZIF-8 under different pressures

Nano ZIF-8 was synthesized according to our previous report [6]. 2 g Zn (NO$_3$)$_2$·6H$_2$O and 5 g 2-methylimidazole (2-MI) were mixed in 200 g methanol. The mixture was kept at 25 °C for 24 h. Then, the product was washed with methanol and dried in vacuum for 48 h.

aZIF-8 were prepared using a hydraulic pellet press with 20 mm diameter die. Nano ZIF-8 (500 mg) was gently stirred in a non-penetrating fluid to disperse lumps before evenly distributing in the die. The press was subjected to load of 0.3, 0.6 or 0.9 GPa for 5 min before recovering the samples. The sample was named as ZIF-8-X GPa.

2.2. Synthesis of aZIF-8/5-Fu by impregnation or under different pressures

5 ml ZIF-8, ZIF-8-0.3 GPa, ZIF-8-0.6 GPa or ZIF-8-0.9 GPa in PBS (pH = 7.4; 4 mg/ml) and 20 mg 5-Fu were mixed by stirring for 72 h in the dark. The samples were collected and freeze-dried. ZIF-8/5-Fu was

gently stirred in a non-penetrating fluid to disperse lumps before evenly distributing in the die. The press was subjected to load of 0.3, 0.6, and 0.9 GPa for 5 min before recovering the samples to obtain aZIF-8/5-Fu under different pressures. Drug loading = w (5-Fu in nano-system)/w (nano-system).

2.3. Drug release from ZIF-8/5-Fu and ZIF-8-0.6 GPa/5-Fu under different conditions in vitro

The drug release from ZIF-8/5-Fu and ZIF-8-0.6 GPa/5-Fu was tested in different conditions at 37 °C under shaking for 24 h (pH = 7.4 + 10% FBS and pH = 5.5). At various time points, a 1 ml solution was taken for analysis and replaced with equal volume of fresh release medium to maintain sink condition. The release concentrations were determined by UV–vis spectroscopy at 270 nm.

2.4. Cell cytotoxicity and uptake of aZIF-8 in vitro

100 μl ECA-109 or MCF-7 cells (10^5/ml) were seeded in 96-well-culture plates for 24 h. The medium was replaced with different concentrations (1.25–100 μg/ml) of ZIF-8, ZIF-8-0.3 GPa, ZIF-8-0.6 GPa, and ZIF-8-0.9 GPa in the culture medium. After another 24 h, the medium was replaced with 1640 medium that was supplemented with 10% CCK-8 and the cells were incubated for another 4 h at 37 °C. The absorbance intensity of every well was measured at 490 nm.

To ensure cell uptake of ZIF-8 and ZIF-8-0.6 GPa in ECA-109 cells, the element mapping of cells was tested by X-ray fluorescence microscopy (XFM) at Shanghai Synchrotron Radiation Facility (SSRF, Shanghai, China) [29]. ECA-109 cells were allowed to grow on films.

(a)

(b)

(c)
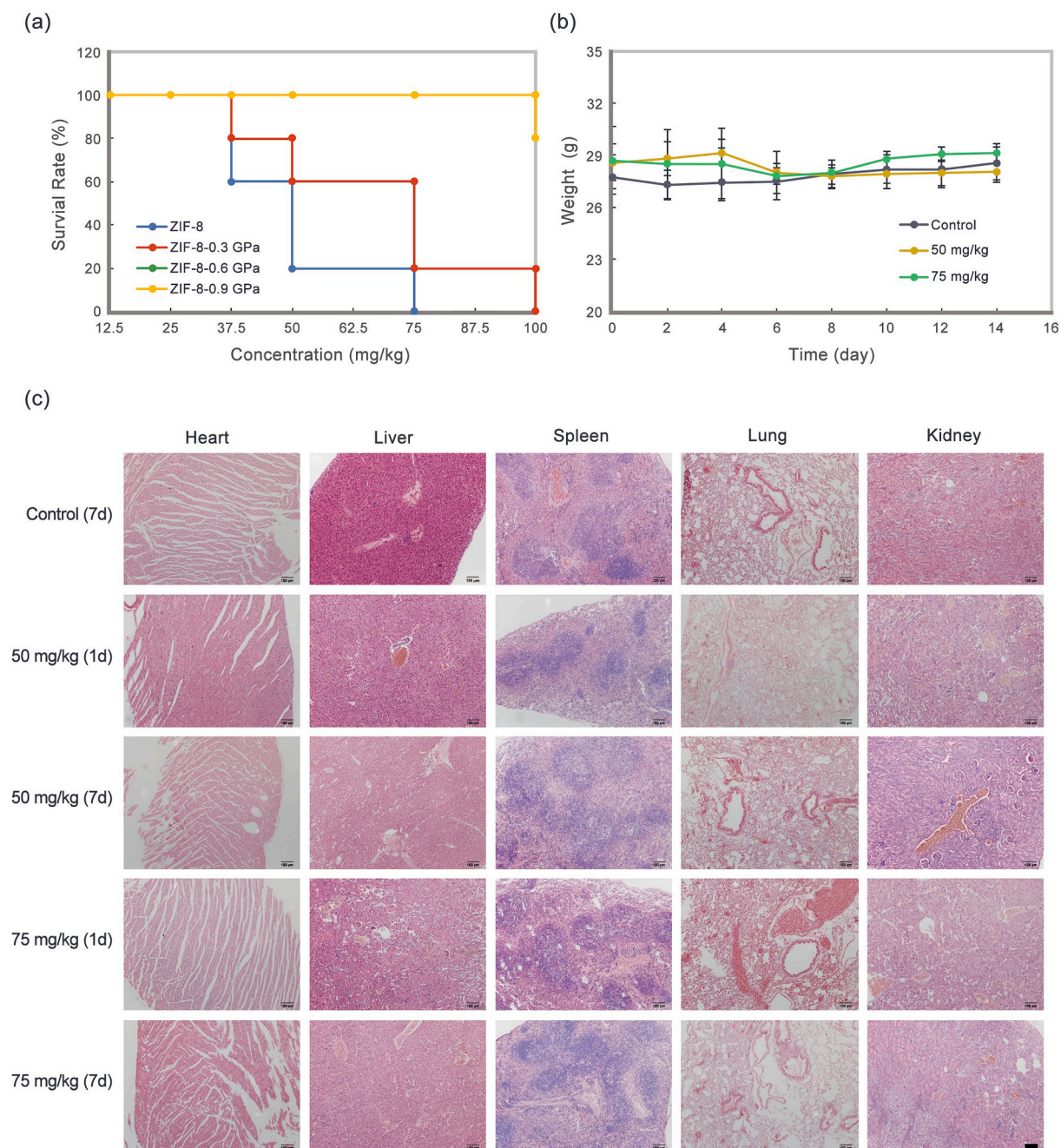
Fig. 3. (a) Survival rate of Balb/c mice after i. v. administration with different dose (12.5, 25, 37.5, 50, 75 and 100 mg/kg) of samples (n = 5) The survival rates of mice were observed for 24 h (The survival rate of ZIF-8-0.6 GPa and ZIF-8-0.9 GPa were same, so the line of ZIF-8-0.6 GPa was covered by the line of ZIF-8-0.9 GPa); (b) Body weight changes after injection with different dosages of ZIF-8-0.6 GPa. Mean ± SD (n = 5); (c) H&E staining of mice major organs injected with 50 and 75 mg/kg ZIF-8-0.6 GPa for 1 or 7 days. (Scale bar = 100 μm).

After 24 h, the cell culture medium was replaced with a new one with ZIF-8 and ZIF-8-0.6 GPa (50 μg/ml), and the cells were incubated for another 4 h. The cells were fixed by tissue fixative before the test. The distribution mapping of elements (Cl and Zn) was assessed by hard X-rays of the BL15U beamline at SSRF. The energy of the X-ray was 15 keV, while the beam spot was 1 × 1 μm/(step*s).

2.5. Toxicity evaluation of aZIF-8 in vivo

The *in vivo* toxicity evaluation was conducted under the approval of the Regional Ethics Committee for Animal Experiments at Ningbo University, China (Permit No. SYXK (Zhe) 2019–0005). For this purpose, mice were randomly injected with ZIF-8, ZIF-8-0.3 GPa, ZIF-8-

0.6 GPa, and ZIF-8-0.9 GPa of different concentrations (12.5, 25, 37.5, 50, 75, and 100 mg/kg, n = 5) via the tail veins. The survival rates of mice were observed for 24 h. Furthermore, 15 mice were randomly divided into three groups and separately injected with PBS, and ZIF-8-0.6 GPa at 50 and 75 mg/kg via the tail veins. The weights of mice were recorded for 14 days. The mice injected with different samples were thereafter sacrificed for histology study of the major organs. The paraffin slices were stained with H&E to verify if there is any damage to the organs.

2.6. Pharmacokinetics and biodistribution of healthy mice in vivo

Mice were administered with ZIF-8 and ZIF-8-0.6 GPa at
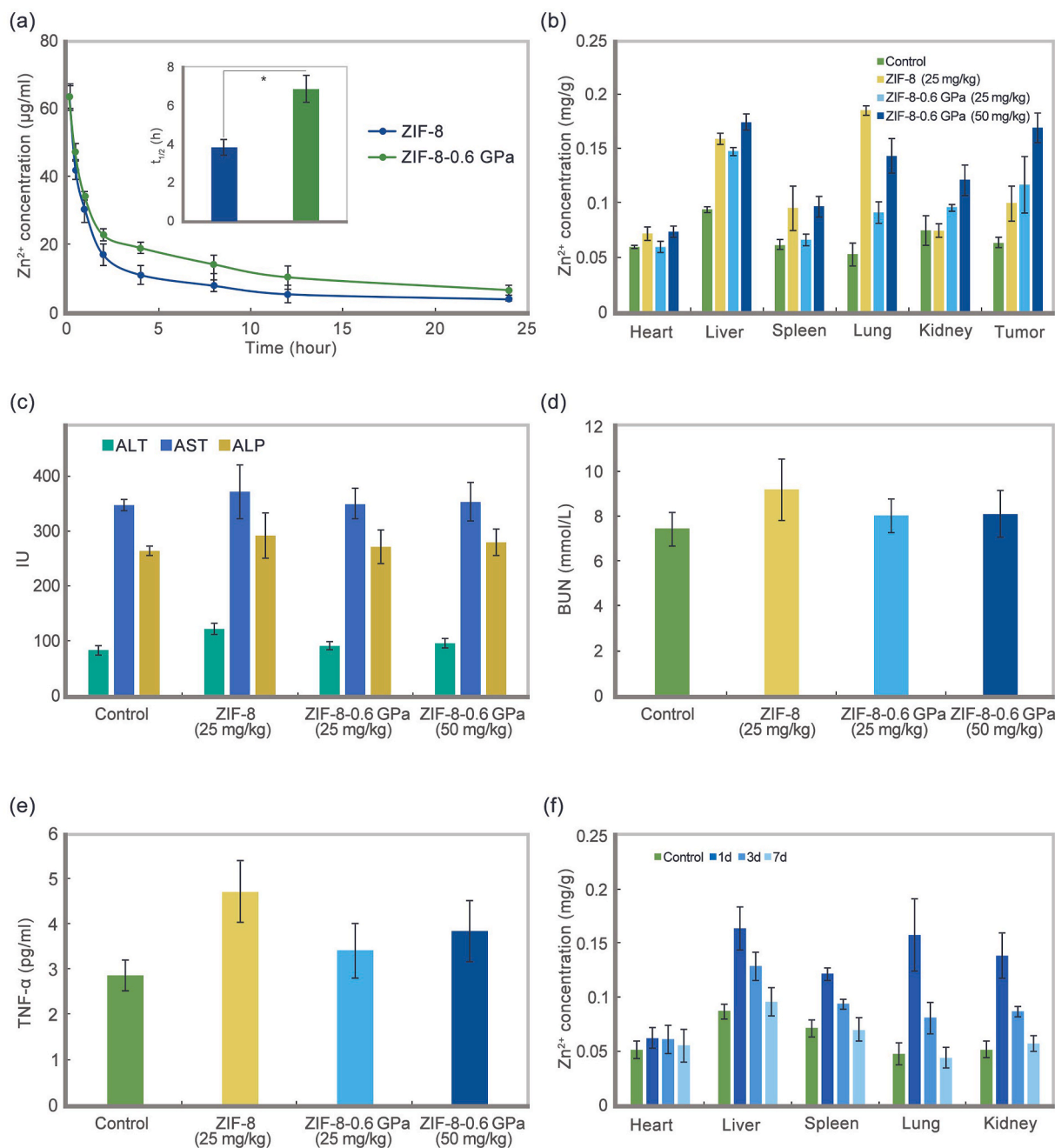
Fig. 4. (a) Blood concentration of Zn^{2+} at different time points after i. v. injection of ZIF-8 and ZIF-8-0.6 GPa (25 mg/kg). Inset is half-life of Zn^{2+} for ZIF-8 and ZIF-8-0.6 GPa Mean $\pm$ SD (n = 3). *, P $<$ 0.05. The pharmacokinetics of Zn^{2+} follows the two-compartment model; (b) Biodistribution of ECA-109 tumor bearing mice after i. v. injection of ZIF-8 (25 mg/kg) and ZIF-8-0.6 GPa (25 and 50 mg/kg) for 24 h. Mean $\pm$ SD (n = 3); (c, d) Serum biochemistry data and (e) TNF-α of healthy mice after i. v. injection of ZIF-8 (25 mg/kg) and ZIF-8-0.6 GPa (25 and 50 mg/kg) for 7 days. Mean $\pm$ SD (n = 3); (f) Biodistribution of health mice after i. v. injection of ZIF-8-0.6 GPa (50 mg/kg) at different times. Mean $\pm$ SD (n = 3).

concentration of 25 mg/kg by intravenous (i.v.) injection. 1 ml blood was collected at various time points (0, 0.17, 0.5, 1, 2, 4, 8, 12, and 24 h) and analyzed by inductively coupled plasma-optical emission spectroscopy (ICP-OES). Mice were also i. v. administered with ZIF-8-0.6 GPa (50 mg/kg). Three mice of one group were randomly sacrificed at 1, 3, and 7 d. The major organs were collected, and the concentration of Zn was tested by ICP-OES.

Additionally, mice were i. v. administered with PBS, ZIF-8 (25 mg/kg), and ZIF-8-0.6 GPa (25 and 50 mg/kg). The blood of mice sacrificed at one day were collected and analyzed by Blood Analyzer (Sysmex XT-1800i, Japan), and Hitachi 7600-110 Autoanalyzer (Hitachi, Tokyo, Japan). TNF-α, IFN-γ, IL-6, and IL-12 were tested by enzyme-linked

immunosorbent assay or ELISA (PBL Biomedical Laboratories and BDBiosciences) according to the manufacturer's instructions.

2.7. The statistics analysis

Statistical analysis was performed by one-way analysis of variance (ANOVA) followed by Student's test with SPSS 18.0 software.
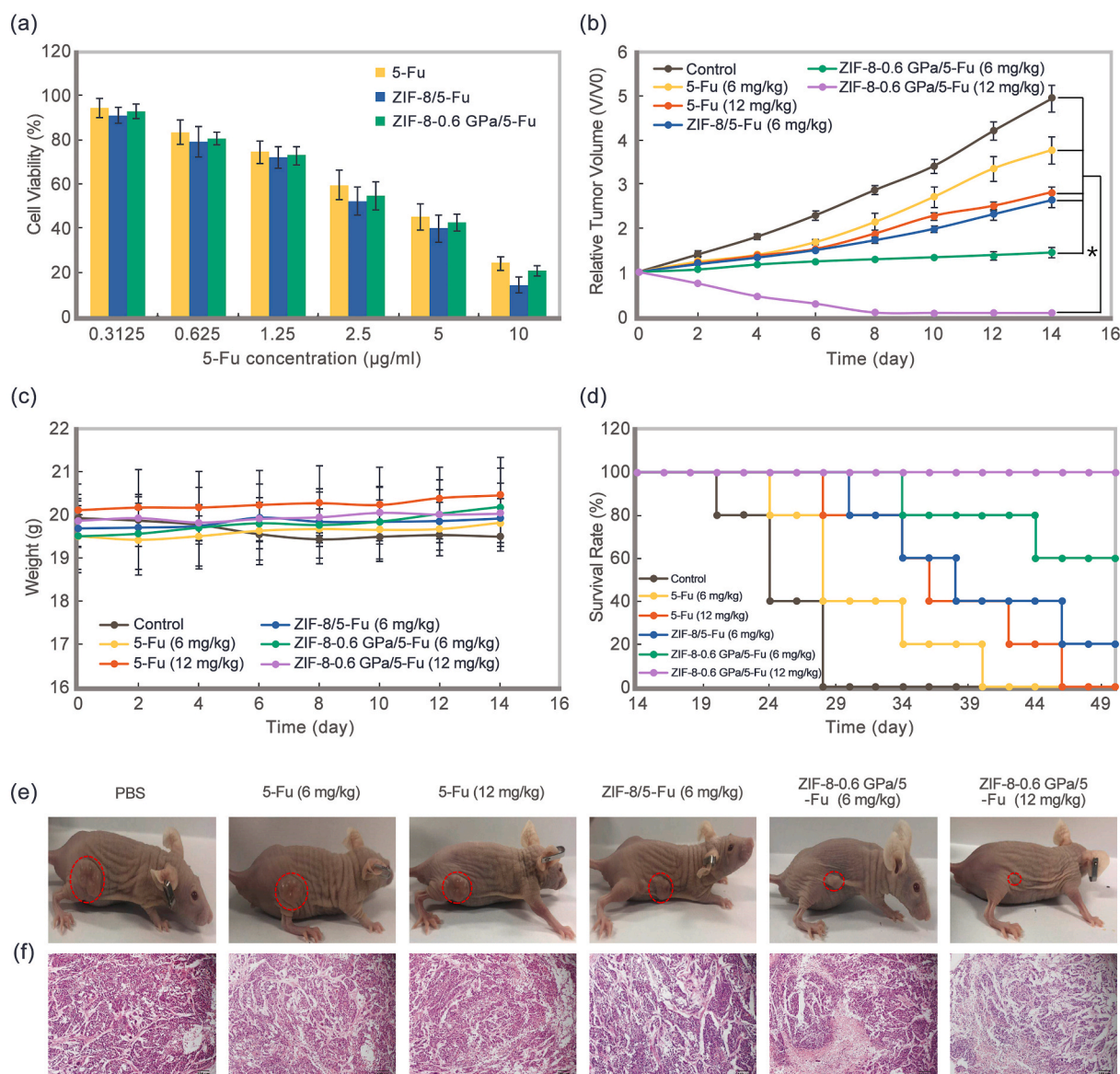
Fig. 5. (a) Cell viability of ECA-109 cells incubated with 5-Fu, ZIF-8/5-Fu, and ZIF-8-0.6 GPa/5-Fu at different concentrations for 24 h. Mean ± SD (n = 3); (b) Relative tumor volume, (c) body weight and (d) survival rate of tumor-bearing mice after treatment with PBS, 5-Fu (6 and 12 mg/kg), ZIF-8/5-Fu (6 mg/kg), and ZIF-8-0.6 GPa/5-Fu (6 and 12 mg/kg). Mean ± SD (n = 5), *, P < 0.05; (e) Photography of tumor-bearing mice 14 days post-injection; (f) H&E staining of tumors for one treatment after 24 h; (Scale bar = 100 μm).

3. Results and discussion

3.1. Characterization of aZIF-8

aZIF-8 was synthesized under different pressures for 5 min. The transmission electron microscopy (TEM) images show that the nano-system becomes irregular after pressure-induction and sizes of the products become a little larger than ZIF-8 (From 85 to 120 nm) (Fig. 1a). From the results of power X-ray diffraction (PXRD) (Fig. 1b and Fig. S1), the intensity of 2θ = 7.5° shows a rapid decrease with the increment of pressure. There are only intensities of 5% remaining after 0.6 GPa and 0.9 GPa, as the collapse pressure of ZIF-8 is 0.34 GPa, which results in irreversible amorphization. Moreover, Fourier transform infrared (FT-IR) spectroscopy shows that the chemical bonds of aZIF-8 are unchanged after the pressure-induction, which indicates the aZIF-8 loses its crystal structure but maintains its chemical structure instead of free metal ions and organic ligand (Fig. 1c). Furthermore, elemental composition shows no obvious change from the results of

organic elemental analysis (Table S1). The sizes of samples in cell culture medium show an obvious increment with increased pressure (Fig. 1d). When the pressure is 0.9 GPa, the size increases to 140 nm from 90 nm, which confirms the results of TEM. The increase in particle size may be due to the collapse of the pores during the pressurization process, which caused the aZIF to fail to maintain a complete frame structure. In addition, the Zeta potentials of all samples show no obvious change after pressure-induced amorphization (Fig. S2). The above results show that aZIF-8 is successfully synthesized under pressure-induced amorphization and maintains the basic connecting blocks and connectivity of ZIF-8 but lacks long-range periodic order.

3.2. Drug loading and toxicity of aZIF-8 in vitro

ZIF-8 has been proven to be an ideal carrier of 5-Fu for its suitable aperture size and specific molecular adsorption [10]. The drug loading was tested by impregnation firstly. All samples were stirred for 3 d with mass ratio of 1:1 (ZIFs to 5-Fu). The results show that the loading

	Heart	Liver	Spleen	Lung	Kidney
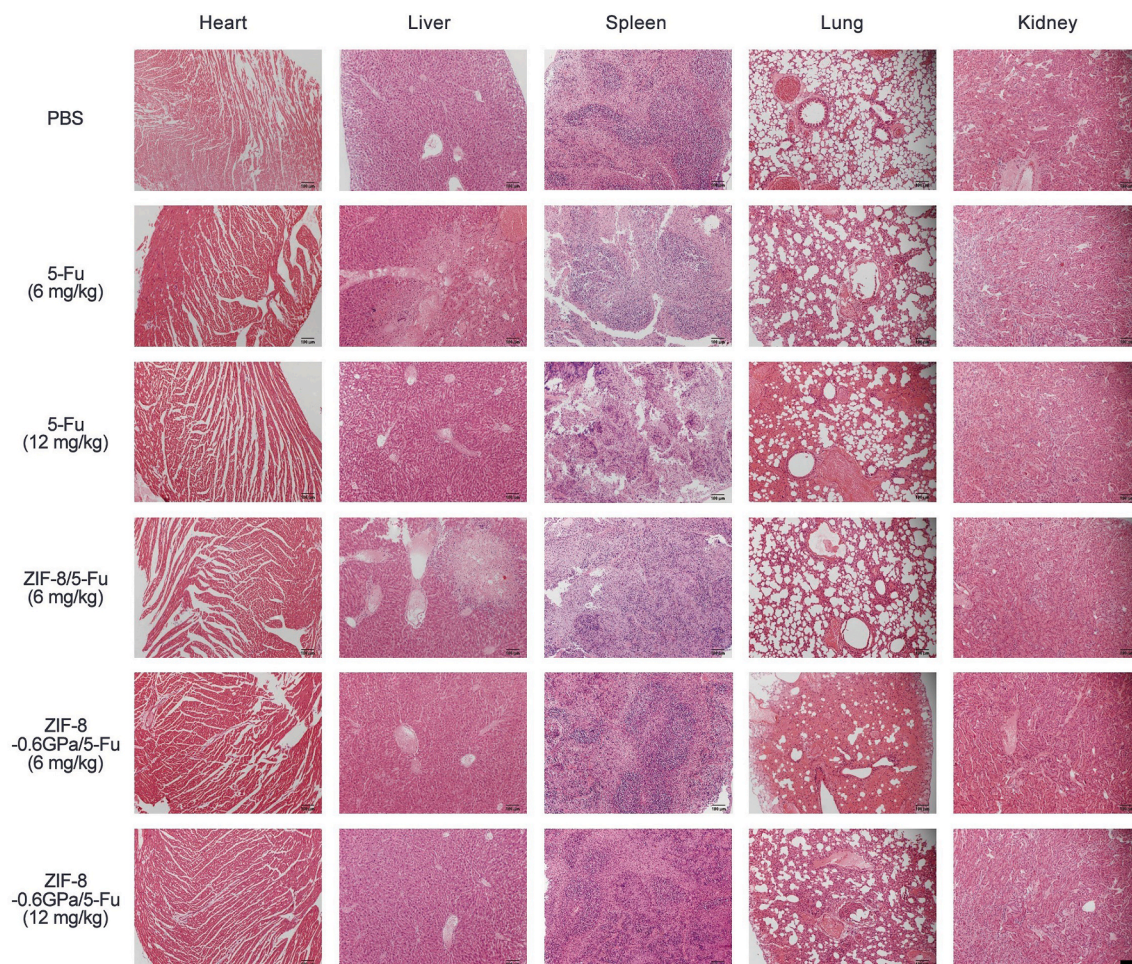
Fig. 6. H&E staining of the major organs of ECA-109 tumor-bearing mice after different treatments for 14 days. (Scale bar = 100 μm).

decreases with increased pressure (Fig. S3). This may be a consequence of the lost long-range periodic order during pressure-induced amorphization, and the BET results also prove this (Fig. S4). To maintain the high drug loading of the nano-system, aZIF-8/5-Fu was synthesized from ZIF-8/5-Fu under pressure-induced amorphization. The drug loading of products shows no obvious decrease under different pressures (Fig. 2a).

Furthermore, the toxicity was tested by CCK-8 in MCF-7 and ECA-109 cells (Fig. 2b and Fig. S5). The toxicity of ZIF-8 and ZIF-8-0.3 GPa increase at concentrations above 40 μg/ml for both cells. On the other hand, ZIF-8-0.6 GPa and ZIF-8-0.9 GPa possess good biocompatibility for both cells at the tested concentrations. A previous report concluded that the release of Zn^{2+} and the enhanced membrane-mediated reactive oxygen species (ROS) production influence the biocompatibility of ZIF-8 [30]. In this regard, Zn^{2+} release in simulation blood for 72 h, and ROS were tested for ZIF-8 and ZIF-8-0.6 GPa as a comparison (Figs. S6 and S7). The ZIF-8-0.6 GPa shows a decrease in Zn^{2+} release within 48 h. The concentration of free Zn^{2+} released in the blood is also lower than the blood concentration [31]. Furthermore, the ZIF-8-0.6 GPa produces less ROS than ZIF-8 after 48 h incubation. Taken the size, drug loading, and toxicity to cells into account, ZIF-8-0.6 GPa was chosen for further exploration and comparison with ZIF-8.

3.3. Drug release and cellular uptake of aZIF-8

Before the evaluation of tumor therapeutic efficacy *in vivo*, drug release and cellular uptake of the nano-system *in vitro* should be tested. As shown in Fig. 2c, both ZIF-8 and ZIF-8-0.6 GPa release

approximately 80% of 5-Fu within 4 h at pH = 5.5, which indicates the amorphous structure does not compromise the pH-sensitivity of Zn–N bonds. This fast drug release in simulated tumor microenvironment could improve therapeutic efficiency. ZIF-8 shows fast 5-Fu release in PBS (pH = 7.4) with 10% FBS within 6 h, which is consistent with previous reports [16]; the fast drug release in the simulated blood environment may reduce its biological outcome. On the other hand, only 30% of 5-Fu is released from ZIF-8-0.6 GPa within 24 h. This is because the subsequent amorphous structure could trap 5-Fu and reduce drug diffusion during circulation. This finding indicates that most of the released drug would be controlled by material degradation for aZIF-8. Furthermore, the decreased drug release during circulation could also minimize the side effects of the free drugs on mice major organs.

To characterize the distribution of elements, X-ray fluorescence microscopy (XRFM) was used to locate the distribution of Zn (Fig. 2 d). The results show that ZIF-8 is only at the point with obvious cluster, while ZIF-8-0.6 GPa disperses throughout the cell with average intensity. A previous report suggests that ZIF-8 tends to intensively accumulate around the membranes [10], however aZIF-8 disperses in cells. The different cellular uptake also reflected the decreased ROS production and the influence of biocompatibility. The cellular uptake amount of ZIF-8-0.6 GPa was also tested for 24 h (Fig. S8). It could be seen that the cellular uptake also increases with increasing incubation concentration, which is consistent with earlier findings on ZIF-8 [10].

As a result, aZIF-8 with high drug loading shows better biocompatibility and less drug release during circulation *in vitro* compared to ZIF-8, which could translate to better biocompatibility and therapeutic effect *in vivo*.

3.4. Biocompatibility of aZIF-8 in vivo

Biocompatibility is one of the main requirements for materials considered in biomedical applications [32]. It refers to the ability of a material to perform its programming functions (such as drug delivery in the human body) without adversely affecting surrounding tissues or altering homeostasis [33]. Acute toxicity experiment *in vivo* was also performed. The safe concentration (without death) is 25 mg/kg for ZIF-8 and ZIF-8-0.3 GPa, and 75 mg/kg for ZIF-8-0.6 GPa and ZIF-8-0.9 GPa (Fig. 3a). In addition, the same survival rate was observed for both ZIF-8-0.6 GPa and ZIF-8-0.9 GPa, which indicated the survival rate did not change with the increase of pressure after amorphization. After the pressure-induced amorphization (P > 0.34 GPa), toxicity of the nano-systems reduces. The body weight changes of mice that were injected with ZIF-8-0.6 GPa through the tail vein were also recorded (Fig. 3b). There is no significant anomaly compared to the control group. The tissue slices of different groups were stained with H&E to determine possible damages induced by ZIF-8-0.6 GPa at different doses (Fig. 3c). There are alveolar collapse and pulmonary bulla in the lung at concentration of 75 mg/kg on the 7th day. Degeneration of the renal tubules and mild steatosis of spleen could be observed at both concentrations on the 1st day. However, the degrees of the lesions improve with time. Additionally, there is normal histology without any hypertrophy or adherent lobes for the liver of all groups. These results show that when the concentration of ZIF-8-0.6 GPa is less than 50 mg/kg, there is no indication of severe toxicity, which provides an insight on the suitable concentrations for further *in vivo* experiments.

3.5. Pharmacokinetics and biodistribution of ZIF-8 and ZIF-8-0.6 GPa in vivo

To better describe ZIF-8-0.6 GPa within the body, series of pharmacokinetic and biodistribution evaluations were conducted and ZIF-8 was set as reference for comparison. The safe concentration of ZIF-8 (25 mg/kg) was used to compare the difference between ZIF-8 and ZIF-8-0.6 GPa. Complementarily, ZIF-8-0.6 GPa at 50 mg/kg was also tested in the biodistribution, biocompatibility, and clearance assessments. At the dose of 25 mg/kg, the serum zinc concentration (Fig. 4a) steadily declines over time for both ZIF-8 and ZIF-8-0.6 GPa. The elimination half-life of ZIF-8-0.6 GPa (6.8 h) is 1.8-fold more than ZIF-8 (3.8 h), indicating the prolonged blood circulation of aZIF-8.

The biodistribution of the nano-systems in tumor-bearing mice was quantified by ICP-OES. The accumulation could be detected in the mice major organs and tumors (Fig. 4b). Most of ZIF-8 are detected in the organs of reticuloendothelial systems (lung, liver and spleen) with high accumulation in the lung, which corresponds to the findings in previous reports [10]. On the contrary, ZIF-8-0.6 GPa shows a different distribution from ZIF-8 at the concentration of 25 mg/kg, as there is an obviously decreased accumulation in the lung and spleen. This may be due to amorphization resulting in the reduction of aZIF accumulation in the lung and kidney. Furthermore, ZIF-8-0.6 GPa shows an increment in the tumor. At concentration of 50 mg/kg, there is a marked increase in all major organs and tumor. These demonstrate that aZIF-8 could increase nano-system accumulation in the tumor by longer circulation time with decreased lung accumulation.

To further understand the effect of the nano-systems on the blood, mice administered with samples were sacrificed after 24 h, and the blood were collected for analysis. No obvious decrease in white blood cells and red blood cells occurs for all groups (Fig. S9). In addition, the biochemistry of blood shows no obvious change among three groups within the normal range (Fig. 4c and d). However, the TNF-α of ZIF-8 shows an increment in comparison with the other three groups (Fig. 4e and Fig. S10). Among those, aZIF-8 exhibits low toxicity and higher tumor accumulation than ZIF-8.

To evaluate the clean-up of aZIF-8 *in vivo*, the major organs of mice were collected at 1, 3, and 7 days after i. v. injection of ZIF-8-0.6 GPa

(50 mg/kg). The concentration of Zn was analyzed by ICP-OES (Fig. 4f). Although there are high accumulations in liver, spleen, lung and kidney, the concentrations obviously decrease with time. Notably, the concentration of ZIF-8-0.6 GPa in the major organs show no obvious difference with the control after 7 days. Due to the non-covalent co-ordination interaction of aZIFs, aZIF could gradually decompose into small molecules and ions which could effectively release out Zn^{2+} in a relatively rapid manner. Further, the ZIF-8-0.6 GPa can be degraded easier than class inorganic materials, and further cleared fast. These therefore establish the rapid clean-up of the aZIFs *in vivo*.

3.6. Anti-tumor effect of ZIF-8 and ZIF-8-0.6 GPa in vitro and in vivo

ECA-109 cells were utilized to investigate the anti-tumor effect of the nano-systems *in vitro*. Both samples exhibit 5-Fu concentration-dependent inhibition of cell proliferation (Fig. 5a). ZIF-8/5-Fu and ZIF-8-0.6 GPa/5-Fu exhibit stronger inhibition than free drug solution. The enhancement of antitumor efficiency might be related to the fast drug release and increased uptake of ZIFs and aZIFs.

An ECA-109-bearing nude mice model was used to evaluate the tumor therapeutic efficacy *in vivo*. The tumor size of treated groups was observed for 14 days after four-time administration. The tumor of ZIF-8-0.6 GPa (12 mg/kg) group grows slowly during treatment and becomes smaller than the original size without recurrence within 14 days (Fig. 5b). Meanwhile, the tumors of other groups grow quickly over time, expect ZIF-8-0.6 GPa (6 mg/kg) that shows no change. H&E staining of the tumor sections post-treatment show that compared to the PBS group, there are much vacuolar chromatin in the ZIF-8-0.6 GPa group. The 5-Fu group only shows increase in the nuclear ratio which indicates no obvious cell necrosis (Fig. 5e and f). It can also be noticed that the survival of ZIF-8-0.6 GPa (12 mg/kg) group is still 100% within 60 days (Fig. 5d). Conversely, the survival of PBS, 5-Fu (6 mg/kg), and 5-Fu (12 mg/kg) groups are zero, while ZIF-8 (6 mg/kg) and ZIF-8-0.6 GPa (6 mg/kg) are 20% and 60%, respectively. The excellent therapeutic efficacy and prolonged survival could be attributed to two major reasons: first, the longer blood circulation time and higher safe concentration leading to higher drug concentration in tumors; second, the fast drug release increases 5-Fu concentration in tumor cells, which consequently induces the cell death.

Furthermore, there is no obvious decrease in body weights during treatment for 14 days (Fig. 5c). In addition, compared to the PBS group (Fig. 6), there is no obvious abnormality in the vital organs for ZIF-8-0.6 GPa-treated group whilst there are obvious damages to liver, spleen, and kidney of the groups treated with free 5-Fu and ZIF-8/5-Fu, corroborating previous H&E results [34]. Taken together, these results indicate that aZIFs enhance tumor therapeutic effect with reduced toxicity, longer blood circulation, and higher accumulation in tumor sites.

4. Conclusion

In this work, pressure-induced aZIF-8/5-Fu was compared with ZIF-8/5-Fu from drug loading, drug release, cell viability, cellular uptake and ROS production *in vitro* to biocompatibility, blood circulation, organs accumulation and therapeutic efficacy *in vivo*. We found that aZIF-8 showed lower drug release in simulation blood environment and better cell biocompatibility than ZIF-8 *in vitro*. In the *in vivo* investigations, aZIF-8 exhibited higher safe concentration, longer blood circulation and higher tumor accumulation with lower lung accumulation. High injection dose and tumor accumulation combined with pH-responsive drug release remarkably improved the therapeutic efficacy of aZIF-8/5-Fu to improve the survival of tumor-bearing mice during and after treatment. Additionally, aZIF-8 showed less side effects on mice major organs and were cleaned up within 14 days at the given dose. Taken together, our study proves that aZIF-8 with favorable biocompatibility, long blood circulation and tumor microenvironment

responsiveness has great potential as a nano-system for effective cancer therapy.

CRediT authorship contribution statement

Zhenqi Jiang: Designing the study, experiments, data collection, interpretation, writing and reviewing manuscript. **Yanying Li:** Experiment, data collection and writing manuscript. **Zhenni Wei:** Data acquisition and analysis. **Bo Yuan:** Design and drawing figures. **Yinjie Wang:** Data analysis. **Ozioma Udochukwu Akakuru:** Revising the manuscript. **Yong Li:** Data acquisition. **Juan Li:** Designing the study, writing, reviewing manuscript and funding acquisition. **Aiguo Wu:** Reviewing, editing the manuscript and funding acquisition.

Declaration of competing interest

The authors declare no competing interests.

Acknowledgements

Appendix A. Supplementary data

Supplementary data to this article can be found online at https://doi.org/10.1016/j.bioactmat.2020.08.036.

References

[1] A. Huang, W. Dou, J. Caro, Steam-stable zeolitic imidazolate framework ZIF-90 membrane with hydrogen selectivity through covalent functionalization, J. Am. Chem. Soc. 132 (44) (2010) 15562–15564.

[2] S.R. Venna, M.A. Carreon, Highly permeable zeolite imidazolate framework-8 membranes for CO2/CH4 separation, J. Am. Chem. Soc. 132 (1) (2010) 76–78.

[3] H.L. Jiang, T. Akita, T. Ishida, M. Haruta, Q. Xu, Synergistic catalysis of Au@Ag Core−Shell nanoparticles stabilized on Metal−Organic framework, J. Am. Chem. Soc. 133 (5) (2011) 1304–1306.

[4] C.G. Jones, V. Stavila, M.A. Conroy, P. Feng, B.V. Slaughter, C.E. Ashley, M.D. Allendorf, Versatile synthesis and fluorescent labeling of ZIF-90 nanoparticles for biomedical applications, ACS Appl. Mater. Interfaces 8 (12) (2016) 7623–7630.

[5] J. Qin, M. Cho, Y. Lee, Ferrocene-encapsulated Zn zeolitic imidazole framework (ZIF-8) for optical and electrochemical sensing of amyloid-β oligomers and for the early diagnosis of alzheimer's disease, ACS Appl. Mater. Interfaces 11 (12) (2019) 11743–11748.

[6] Z. Jiang, Y. Wang, L. Sun, B. Yuan, Y. Tian, L. Xiang, Y. Li, Y. Li, J. Li, A. Wu, Dual ATP and pH responsive ZIF-90 nanosystem with favorable biocompatibility and facile post-modification improves therapeutic outcomes of triple negative breast cancer in vivo, Biomaterials 197 (2019) 41–50.

[7] Z. Jiang, B. Yuan, N. Qiu, Y. Wang, L. Sun, Z. Wei, Y. Li, J. Zheng, Y. Jin, Y. Li, S. Du, J. Li, A. Wu, Manganese-zeolitic imidazolate frameworks-90 with high blood circulation stability for MRI-guided tumor therapy, Nano-Micro Lett. 11 (1) (2019) 61.

[8] J. Della Rocca, D. Liu, W. Lin, Nanoscale metal–organic frameworks for biomedical imaging and drug delivery, Acc. Chem. Res. 44 (10) (2011) 957–968.

[9] A. Phan, C.J. Doonan, F.J. Uribe-Romo, C.B. Knobler, M. O'Keeffe, O.M. Yaghi, Synthesis, structure, and carbon dioxide capture properties of zeolitic imidazolate frameworks, Acc. Chem. Res. 43 (1) (2010) 58–67.

[10] S. Li, K. Wang, Y. Shi, Y. Cui, B. Chen, B. He, W. Dai, H. Zhang, X. Wang, C. Zhong, H. Wu, Q. Yang, Q. Zhang, Novel biological functions of ZIF-NP as a delivery vehicle: high pulmonary accumulation, favorable biocompatibility, and improved therapeutic outcome, Adv. Funct. Mater. 26 (16) (2016) 2715–2727.

[11] Z. Xie, X. Cai, C. Sun, S. Liang, S. Shao, S. Huang, Z. Cheng, M. Pang, B. Xing, A.A.A. Kheraif, J. Lin, O2-Loaded pH-responsive multifunctional nanodrug carrier for overcoming hypoxia and highly efficient chemo-photodynamic cancer therapy, Chem. Mater. 31 (2) (2018) 483–490.

[12] J. Zhuang, C.-H. Kuo, L.-Y. Chou, D.-Y. Liu, E. Weerapana, C.-K. Tsung, Optimized metal–organic-framework nanospheres for drug delivery: evaluation of small-molecule encapsulation, ACS Nano 8 (3) (2014) 2812–2819.

[13] X. Lian, Y. Fang, E. Joseph, Q. Wang, J. Li, S. Banerjee, C. Lollar, X. Wang, H.-C. Zhou, Enzyme-MOF (Metal-Organic framework) composites, Chem. Soc. Rev. 46 (11) (2017) 3386–3401.

[14] Q. Sun, Z. Zhou, N. Qiu, Y. Shen, Rational Design of cancer nanomedicine: nano-property integration and synchronization, Adv. Mater. 29 (14) (2017) 1606628-n/a.

[15] T. Du, C. Zhao, F. ur Rehman, L. Lai, X. Li, Y. Sun, S. Luo, H. Jiang, N. Gu, M. Selke, X. Wang, In situ multimodality imaging of cancerous cells based on a selective performance of Fe2+-adsorbed zeolitic imidazolate framework-8, Adv. Funct. Mater. 27 (5) (2017) 1603926-n/a.

[16] Q. Wu, M. Niu, X. Chen, L. Tan, C. Fu, X. Ren, J. Ren, L. Li, K. Xu, H. Zhong, X. Meng, Biocompatible and biodegradable zeolitic imidazolate framework/polydopamine nanocarriers for dual stimulus triggered tumor thermo-chemotherapy, Biomaterials 162 (2018) 132–143.

[17] L. Su, Q. Wu, L. Tan, Z. Huang, C. Fu, X. Ren, N. Xia, Z. Chen, X. Ma, X. Lan, Q. Zhang, X. Meng, High biocompatible ZIF-8 coated by ZrO2 for chemo-microwave thermal tumor synergistic therapy, ACS Appl. Mater. Interfaces 11 (11) (2019) 10520–10531.

[18] R. Gaillac, P. Pullumbi, K.A. Beyer, K.W. Chapman, D.A. Keen, T.D. Bennett, F.-X. Coudert, Liquid metal–organic frameworks, Nat. Mater. 16 (2017) 1149.

[19] T.D. Bennett, A.K. Cheetham, Amorphous metal–organic frameworks, Acc. Chem. Res. 47 (5) (2014) 1555–1562.

[20] S. Conrad, P. Kumar, F. Xue, L. Ren, S. Henning, C. Xiao, K.A. Mkhoyan, M. Tsapatsis, Controlling dissolution and transformation of zeolitic imidazolate frameworks by using electron-beam-induced amorphization, Angew. Chem. Int. Ed. 57 (41) (2018) 13592–13597.

[21] S. Cao, T.D. Bennett, D.A. Keen, A.L. Goodwin, A.K. Cheetham, Amorphization of the prototypical zeolitic imidazolate framework ZIF-8 by ball-milling, Chem. Commun. 48 (63) (2012) 7805–7807.

[22] K.W. Chapman, G.J. Halder, P.J. Chupas, Pressure-induced amorphization and porosity modification in a Metal−Organic framework, J. Am. Chem. Soc. 131 (48) (2009) 17546–17547.

[23] T.D. Bennett, S. Horike, Liquid, glass and amorphous solid states of coordination polymers and metal–organic frameworks, Nat. Rev. Mater. 3 (11) (2018) 431–440.

[24] K.W. Chapman, D.F. Sava, G.J. Halder, P.J. Chupas, T.M. Nenoff, Trapping guests within a nanoporous metal–organic framework through pressure-induced amorphization, J. Am. Chem. Soc. 133 (46) (2011) 18583–18585.

[25] A. Kertik, L.H. Wee, M. Pfannmöller, S. Bals, J.A. Martens, I.F.J. Vankelecom, Highly selective gas separation membrane using in situ amorphised metal–organic frameworks, Energy Environ. Sci. 10 (11) (2017) 2342–2351.

[26] S. Horike, W. Chen, T. Itakura, M. Inukai, D. Umeyama, H. Asakura, S. Kitagawa, Order-to-Disorder structural transformation of a coordination polymer and its influence on proton conduction, Chem. Commun. 50 (71) (2014) 10241–10243.

[27] C. Orellana-Tavra, E.F. Baxter, T. Tian, T.D. Bennett, N.K.H. Slater, A.K. Cheetham, D. Fairen-Jimenez, Amorphous metal–organic frameworks for drug delivery, Chem. Commun. 51 (73) (2015) 13878–13881.

[28] S.A. Moggach, T.D. Bennett, A.K. Cheetham, The effect of pressure on ZIF-8: increasing pore size with pressure and the formation of a high-pressure phase at 1.47 GPa, Angew. Chem. Int. Ed. 48 (38) (2009) 7087–7089.

[29] Z. Jiang, Y. Tian, D. Shan, Y. Wang, E. Gerhard, J. Xia, R. Huang, Y. He, A. Li, J. Tang, H. Ruan, Y. Li, J. Li, J. Yang, A. Wu, pH protective Y1 receptor ligand functionalized antiphagocytosis BPLP-WPU micelles for enhanced tumor imaging and therapy with prolonged survival time, Biomaterials 170 (2018) 70–81.

[30] M. Hoop, C.F. Walde, R. Riccò, F. Mushtaq, A. Terzopoulou, X.-Z. Chen, A.J. deMello, C.J. Doonan, P. Falcaro, B.J. Nelson, J. Puigmartí-Luis, S. Pané, Biocompatibility characteristics of the metal organic framework ZIF-8 for therapeutical applications, Appl. Mater. Today 11 (2018) 13–21.

[31] G. Lusvardi, G. Malavasi, L. Menabue, M.C. Menziani, A. Pedone, U. Segre, V. Aina, A. Perardi, C. Morterra, F. Boccafoschi, S. Gatti, M. Bosetti, M. Cannas, Properties of zinc releasing surfaces for clinical applications, J. Biomater. Appl. 22 (6) (2008) 505–526.

[32] P. Horcajada, R. Gref, T. Baati, P.K. Allan, G. Maurin, P. Couvreur, G. Férey, R.E. Morris, C. Serre, Metal–organic frameworks in biomedicine, Chem. Rev. 112 (2) (2012) 1232–1268.

[33] D.F. Williams, On the mechanisms of biocompatibility, Biomaterials 29 (20) (2008) 2941–2953.

[34] X. Sun, R. Du, L. Zhang, G. Zhang, X. Zheng, J. Qian, X. Tian, J. Zhou, J. He, Y. Wang, Y. Wu, K. Zhong, D. Cai, D. Zou, Z. Wu, A pH-responsive yolk-like nanoplatform for tumor targeted dual-mode magnetic resonance imaging and chemotherapy, ACS Nano 11 (7) (2017) 7049–7059.